nature photonics

Review article

https://doi.org/10.1038/s41566-026-02010-1

Solution-processed nano-LEDs for next-generation optoelectronic technologies

Received: 9 May 2026

Accepted: 6 August 2026

Published online: 21 October 2026

Check for updates

Wenqiang Yang[1,2,3,10], Aobo Ren[4,10], Xiaoyu Yang[5,10], Hao Wang[6,7,10], Tae-Woo Lee[8,9] ✉ & Deying Luo[1] ✉

Light-emitting diodes (LEDs), with pixel sizes ranging from the millimetre to micrometre scale, have driven advances in display technologies for large-area panels, portable devices and wearable platforms. As applications expand beyond conventional displays to optical sensing, implantable optogenetics, on-chip optical interconnects and super-resolution microscopy, demand is growing for ultracompact, energy-efficient light sources capable of subwavelength and spatiotemporal control. Nanoscale light-emitting diodes (nano-LEDs) stand out as promising candidates to address these requirements, offering exceptional control over light generation, confinement and emission dynamics. Here we discuss recent progress in colloidal quantum dots and perovskite nano-LED technologies across material chemistry, device engineering and nanofabrication strategies. We also propose future research directions for harnessing nano-LEDs in emerging applications, underscoring their potential to move beyond traditional optoelectronic functions. Far beyond a miniaturized extension of conventional LEDs, nano-LEDs are poised to become a transformative platform uniting optoelectronics, nanophotonics and device engineering.

Advances in light-emitting diodes (LEDs) with pixel sizes from millimetres to micrometres have transformed modern light sources and display technologies. However, as visual and functional requirements continue to rise, conventional LEDs increasingly fall short of meeting the demands of emerging applications for higher pixel densities and multifunctional operation. Active-matrix addressing has overcome this limitation by enabling LEDs to operate as high-density, individually controlled light-emitting systems in high-density arrays. Driven by a relentless demand for higher spatial resolution and data bandwidth, this technology has steadily scaled LED pixel sizes down from the millimetre to the micrometre regime. In their current form, micro-LEDs based on diverse material platforms[1,2] have achieved densities above 2,000 pixels per inch (PPI) as they approach the ~1-μm dimensional threshold[3]. Although this miniaturization trajectory initially catalysed the evolution of visual interfaces—spanning from large-format screens to emerging near-eye display technologies[4]—its impact now extends far beyond traditional displays (Fig. 1).

The push for higher pixel densities and greater device functionality is driving LEDs to ever-smaller nanoscale dimensions (referred to here as nano-LEDs), creating opportunities in high-speed light fidelity, on-chip optical interconnects and spatially localized optogenetics. Distinct from nanowire LEDs, which utilize semiconductor nanowires as the emissive layer[5], nano-LEDs refer here to electrically driven LEDs in which the emissive region or pixel pitch is reduced to

[1]International Institute for Interdisciplinary and Frontiers, Beihang University, Beijing, China. [2]Institute of Atomic Manufacturing, Beihang University, Beijing, China. [3]Hangzhou International Innovation Institute, Beihang University, Hangzhou, China. [4]Institute of Fundamental and Frontier Sciences, University of Electronic Science and Technology of China, Chengdu, China. [5]State Key Laboratory for Mesoscopic physics and Frontiers Science Center for Nano-optoelectronics, School of Physics, Peking University, Beijing, China. [6]Centre for Photonic Systems, Department of Engineering, University of Cambridge, Cambridge, UK. [7]School of Instrumentation and Optoelectronic Engineering, Beihang University, Beijing, China. [8]Department of Materials Science and Engineering, Seoul National University, Seoul, Republic of Korea. [9]Soft Foundry, Research Institute of Advanced Materials, Institute of Engineering Research, Interdisciplinary Program in Bioengineering, Seoul National University, Seoul, Republic of Korea. [10]These authors contributed equally: Wenqiang Yang, Aobo Ren, Xiaoyu Yang, Hao Wang. ✉e-mail: twlees@snu.ac.kr; bhldy@buaa.edu.cn

https://doi.org/10.1038/s41566-026-02010-1

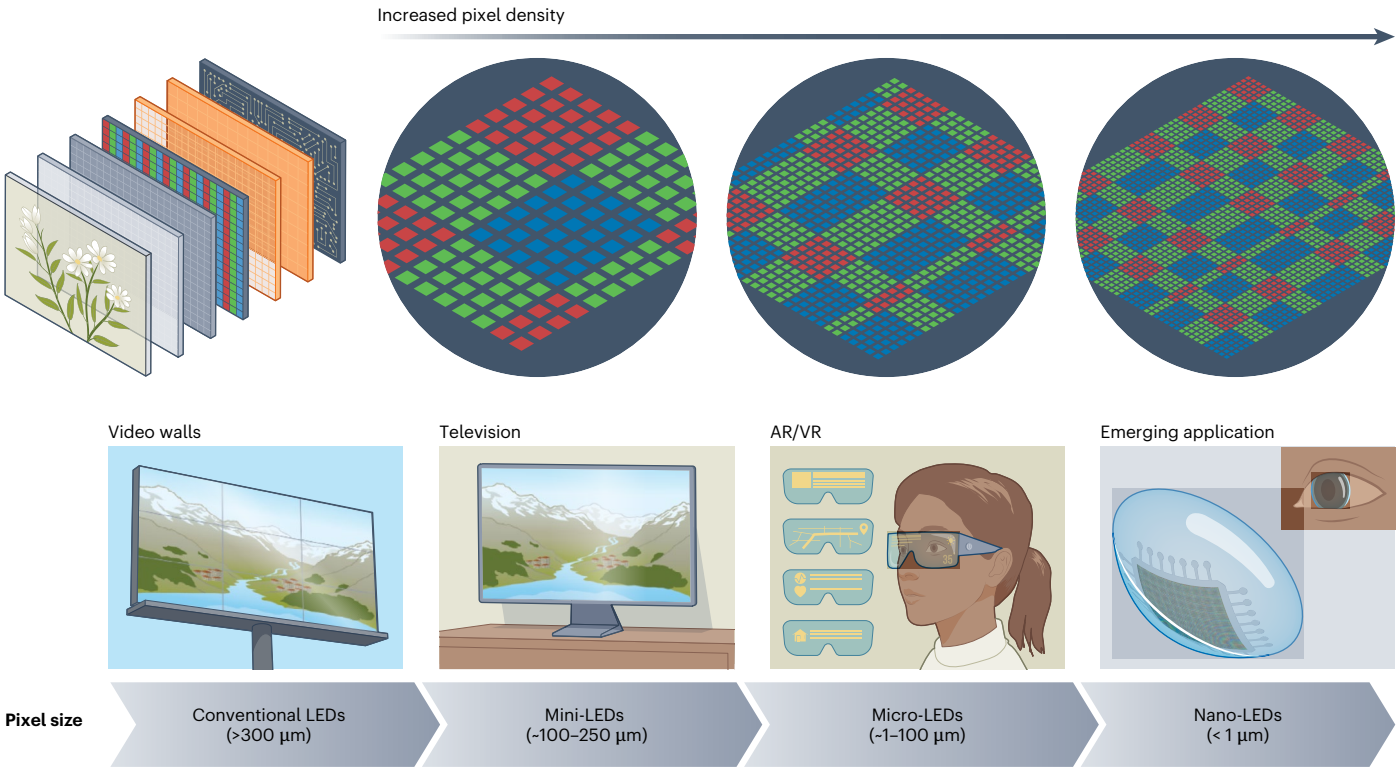


Fig. 1 | Pixel densities continue to increase with the development of LED technology for different application scenarios. Conventional LEDs (pixel size > 300 μm) are widely used in indoor and outdoor video walls. Mini-LEDs (pixel size ~100–250 μm) are adopted in televisions and in-car displays. Micro-LEDs (pixel size ~1–100 μm) are employed in mobile electronics and AR/VR displays. For emerging applications such as implantable photonics, holographic projection and neuroscience, nano-LEDs with pixel sizes <1 μm are increasingly needed.

the submicrometre regime, typically approaching or falling below the optical wavelength. By shrinking the active emissive region, such nano-LEDs offer strong spatial confinement, a high local density of optical states, and a structurally minimized geometric capacitance. This transition not only enables unprecedented pixel densities exceeding 10,000 PPI (ref. 6), but intrinsically lowers energy consumption and unlocks the ultrafast modulation speed required for chip-scale photonic integration, highly localized optogenetic neural interfaces, and emerging photonic technologies[7–10]. Therefore, nano-LEDs are promising for next-generation ultrahigh-resolution and compact electronic systems.

Despite their considerable potential, nano-LEDs have yet to deliver, in a single platform, ultrahigh pixel density, high efficiency, long operational lifetime and scalable full-colour integration[11–13]. As pixel dimensions enter the submicrometre regime, sidewall and interfacial defects, carrier losses and fabrication-induced non-uniformity increasingly compromise device performance, meaning that aggressive size downscaling often comes at the cost of efficient electroluminescence (EL). For instance, organic LEDs (OLEDs) on silicon backplanes exhibit pronounced efficiency roll-off at submicrometre pixel dimensions, as the high current densities required for high luminance exacerbate unbalanced carrier transport and exciton quenching[14,15]. In this context, selecting appropriate material systems, fabrication methods and heterogeneous integration strategies is critical to realizing efficient and stable nano-LEDs.

Solution-processed colloidal quantum dots (QDs) and halide perovskites offer a distinct route towards nano-LEDs, complementary to established III–V and organic emitters. Their appeal lies in the combination of low-temperature processability, high photoluminescence (PL) quantum yield (QY), compositionally tunable emission and narrow emission linewidths[16–18]. Beyond these attributes, these material systems offer access to engineered nanocrystal solids, superlattices, multiple-quantum-well structures and pixelated emissive architectures, enabling spatial confinement over nanoscale dimensions[19,20]. Such features enable enhanced spontaneous emission rates, rapid modulation and low latency, characteristics that are particularly advantageous for coherent light sources[21,22]. Moreover, nano-LED arrays based on colloidal QDs and halide perovskites that are suitably integrated with optical cavities can generate coherent light suitable for advanced optical imaging and neural-interface applications, including super-resolution microscopy, optogenetic stimulation and single-cell-resolution optical recording of resolution[23,24]. The ultracompact footprint of nano-LEDs also permits direct integration with nanoscale photonic cavities, waveguides and antennas, thereby facilitating the development of electrically pumped nano-lasers for coherent light sources in future information technologies[25]. Additionally, there are also numerous cutting-edge applications that urgently need high-performance nano-LEDs, such as implantable diagnostic photonics, holographic projectors, laser beam scanning systems and so on[26,27].

In this Review, we trace the trajectory of light-emitting technologies from macroscopic applications to the current frontier of extreme pixel miniaturization. We focus specifically on the emerging paradigm of colloidal QDs and halide perovskite systems. We critically examine how the outstanding optoelectronic properties and solution processability of these nanomaterials inform miniaturized device architectures and advanced nanofabrication strategies. Finally, we outline the roadmap for pushing these high-performance nano-LEDs towards next-generation frontiers in the future.

Fundamentals of nano-LED devices

As LED dimensions shrink into the nanoscale regime, where they exhibit potentially outstanding optoelectronic properties compared with micro-LEDs (Fig. 2a), the surrounding electromagnetic environment is no longer merely a passive optical boundary, but instead becomes

https://doi.org/10.1038/s41566-026-02010-1

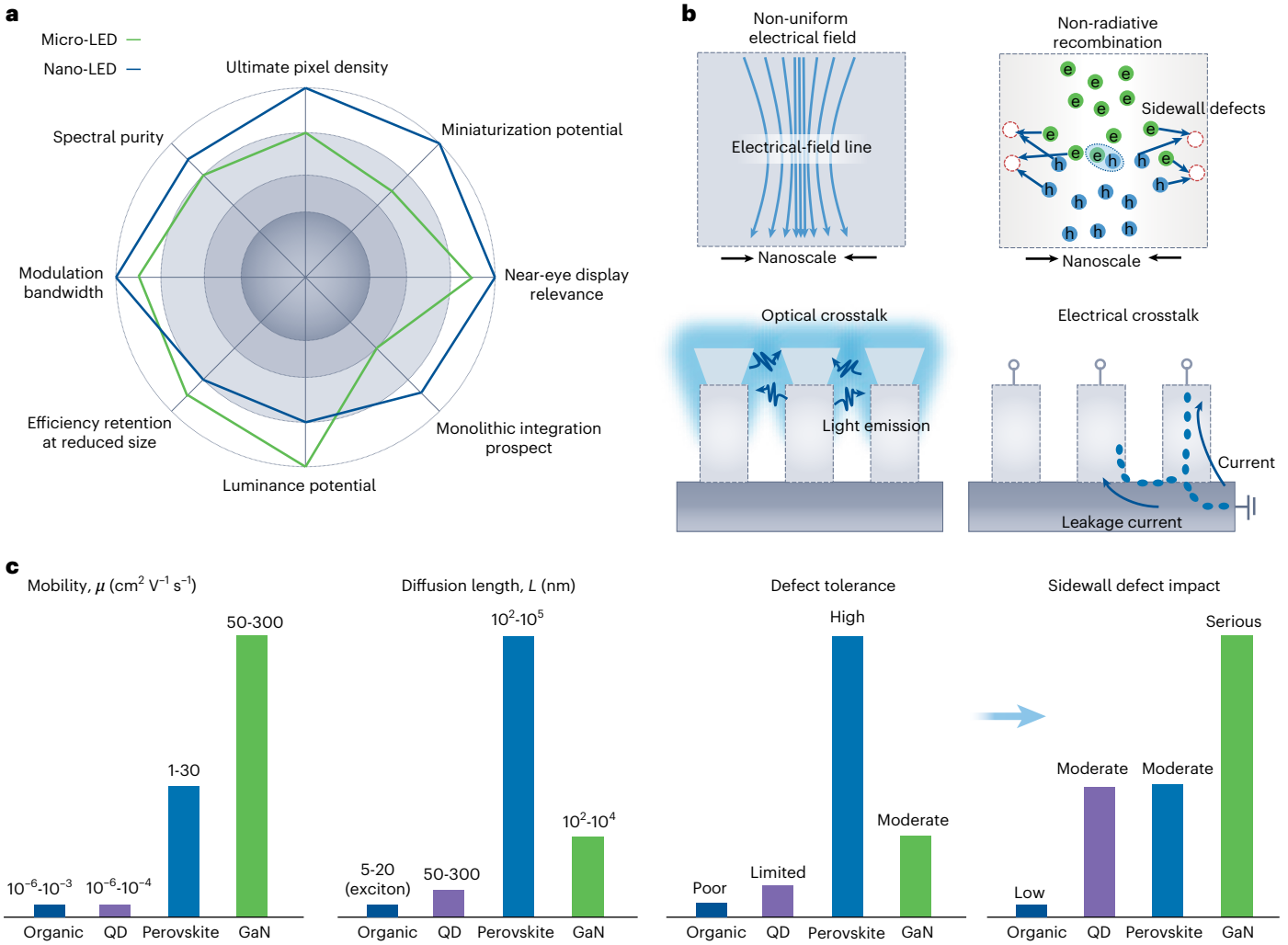


Fig. 2 | Impact of a sidewall defect in nano-LEDs. a, Radar plot comparing micro-LED and nano-LED technologies across several key performance dimensions. **b**, Sidewall defects induce challenges in nano-LEDs. **c**, Key parameters that determine the sidewall defect impact on the performance of nano-LEDs based on diverse emission materials, including organic materials, QDs, perovskites and GaN.

an integral part of device operation. Optical modes can be compressed into subwavelength volumes by nanocavities, high-index dielectric resonators, or hybrid metal–dielectric structures, resulting in enhanced field intensity[28]. Such high field intensity can modify the spontaneous emission rate, reshape spectral features, and redirect photons into selected radiation or guided modes through Purcell-type effects[29]. Furthermore, nanoscale geometries enable local optical mode engineering. For example, antenna-like modes can control emission directionality and outcoupling from nanoscale emitters[30]. However, translating these photonic advantages into practical nano-LEDs requires that nanoscale optical-mode control must be matched with equally precise electrical design, because the ultimate performance of nano-LEDs still depends on how efficiently carriers are injected, transported and converted into photons within such confined geometries.

To fulfil the potential of nano-LEDs, nanoscale device architectures must be coupled with improved efficiency, stability and operational reliability. Efficient charge-carrier injection at these interfaces, balanced charge transport across nanoscale pixels, and radiative recombination within the emissive zone where injected holes and electrons meet collectively dictate device performance. However, miniaturized pixels fabricated by sidewall etching exhibit substantially higher surface-to-volume ratios than their larger counterparts[11], so defects at the sidewalls and top surfaces of the emissive layers can impede charge-carrier injection owing to unfavourable energy-band alignment at the emissive/charge-transport layer interfaces. A high density of sidewall defects is also widely regarded as the dominant source of non-radiative recombination[31]. The resulting surface band bending and trap-assisted carrier losses degrade electrical uniformity, producing spatially nonuniform current distribution, local current crowding and unstable carrier confinement across the active region[32]. Furthermore, in high-density nano-LED arrays, sidewall defects also facilitate lateral leakage and parasitic conduction between neighbouring pixels, leading to electrical crosstalk[32], while imperfect optical confinement and sidewall-induced scattering promote lateral photon spreading and optical crosstalk[33,34]. Therefore, sidewall defects are not merely a fabrication imperfection, but a central bottleneck that combines efficiency degradation, poor electrical uniformity, optical crosstalk and inter-pixel interference (Fig. 2b). As a result, the key question for high-performance nano-LED development is not simply which materials perform well in conventional LEDs, but which materials can better tolerate or mitigate the sidewall defect penalty associated with aggressive lateral downscaling.

We therefore investigated surface recombination and other key parameters that determine the performance metrics of nano-LEDs (Fig. 2c). Yapparov and colleagues demonstrated compelling PL imaging evidence showing that carrier recombination is strongly suppressed near damaged sidewall regions, directly confirming the loss of active light-emitting area due to surface defects[35]. In addition, Shen et al.

presented a simple analytical expression describing the influence of reduced lateral dimensions on the radiative recombination rate $R(x)$ along the x direction in micro- and nano-LEDs[36]:

$$R(x) = \mathrm{A}\ \exp\left(-\frac{|x - x_{\mathrm{C}}|}{L}\right) \quad (1)$$

$$L = \sqrt{D\tau} \quad (2)$$

$$D = \frac{k_{\mathrm{B}}T}{e}\mu \quad (3)$$

where x_{C} is the recombination centre, L is the carrier diffusion length, D is the minority-carrier diffusion coefficient, τ is the minority-carrier lifetime, μ is the minority-carrier mobility, k_{B} is the Boltzmann constant and T is the temperature. Although a long carrier diffusion length can support efficient radiative recombination in defect-free regions, it can also increase the probability that carriers diffuse laterally to defect-rich sidewalls. This relation indicates that once the lateral dimension of a nano-LED approaches the carrier diffusion length, an increasing fraction of injected carriers can reach defect-rich sidewalls, enhancing non-radiative recombination losses. Consequently, these sidewall defects are no longer peripheral perturbations; instead, they dominate the electrostatic field, carrier transport and non-radiative recombination of the entire pixel. In addition, sidewall effects can couple with other failure mechanisms, such as unbalanced carrier injection, Joule heating and Auger annihilation, exacerbating the device degradation. Unbalanced carrier injection can promote carrier accumulation and trap-assisted recombination near defective sidewalls[37], while Joule heating accumulation in high-density arrays may activate sidewall traps and accelerate interfacial degradation[38]. In addition, the reduced emissive volume increases local exciton or carrier density, enhancing exciton–exciton, exciton–polaron or Auger-type annihilation near defect-rich regions[39].

Charge-carrier transport characteristics, including charge-carrier mobility and diffusion lengths, are central to surface recombination as device dimensions are scaled down to the nanoscale. Because the energetic nature of surface states and diffusion lengths differ across semiconductor material systems, the associated surface-recombination velocities also vary accordingly. In organic semiconductors, the extremely short (~10 nm) diffusion length of tightly bound Frenkel excitons makes recombination at sidewalls negligible[40]. Despite their widespread use in smartphones and vritual reality (VR) headsets, OLEDs also exhibit degraded electroluminescent performance when scaled to nanoscale pixels, with reduced luminance, external quantum efficiency and uniformity. Although this class of organic nanoscale emissive pixels is largely free of sidewall defects, the diminished operational performance of these devices instead probably stems from accelerated exciton annihilation associated with charge trapping, charge imbalance, exciton–polaron quenching and excited-state chemical degradation[41,42]. Notably, pixel miniaturization reduces the effective radiative recombination volume, leading to substantial efficiency degradation[15,43,44]. By contrast, the sidewall surfaces of conventional GaN emissive materials exhibit higher defect densities that serve as the primary source of performance loss in nano-LEDs. GaN-based semiconductors possess high mobility and long carrier diffusion lengths[45–47], which exacerbate non-radiative recombination at sidewall regions. Importantly, current passivation strategies cannot efficiently passivate the sidewall defects in nano-LEDs based on III–V nitride[48]. Hence, extreme pixel miniaturization in III–V nitride LEDs faces a notable challenge in reducing performance losses arising from defects on nanoscale sidewalls. It is clear that the optoelectronic properties of nanoscale emissive pixels are governed primarily by the choice of emissive material, as the inherent properties of these materials—together with the processing methods used to pattern them into nanoscale pixels—determine the impact of sidewall defects (Fig. 2c). In this context, screening emissive materials compatible with nano-LED requirements remains critical for advancing the technology.

Halide perovskites and QDs offer both broad optoelectronic tunability and processing flexibility[49–52]. Unlike conventional epitaxial semiconductors, these solution-processable materials offer alternative, additive patterning strategies. Techniques such as direct photolithography and transfer printing completely bypass etch-induced surface damage. Hence, when patterned into nano-LEDs, these two materials can mitigate performance losses arising from sidewall defects, severe interfacial recombination and insufficient carrier injection, enabled by the precise surface-chemistry modification and inactive localized contacts that can suppress sidewall non-radiative recombination and crosstalk between neighbouring pixels. QDs, colloidal nanocrystals with engineered surface chemistries, provide exceptional flexibility in tuning optoelectronic properties[53]. Through precise surface-chemistry modification, effective surface ligands can help mitigate sidewall defects[54]. However, improper ligand choice compromises the electrical properties of nano-LEDs. Halide perovskites, another class of emerging emissive semiconductors, have been incorporated into micro- and nano-LEDs, exhibiting alleviated efficiency drop when pixels are downscaled to the nanometre regime[44]. This mitigation of device performance degradation in nano-LEDs arises from reduced sidewall defects via a combined effect of bottom–up growth processing on a localized contact passivation template[55]. Moreover, halide perovskite emissive materials exhibit high defect tolerance[56], balanced charge-carrier diffusion lengths, and tunable emission wavelengths, achieved by varying the composition and exploiting quantum-confinement effects[57,58]. Overall, QDs and halide perovskites stand out as particularly attractive platforms for nano-LEDs, motivating the focus of this Review on recent progress in nano-LEDs based on QDs and perovskites.

Research progress on nano-LEDs based on QDs and perovskites

Notable advances in materials design, fabrication strategies and device architecture have mitigated electrical and optical losses, enabling appreciable performance improvements in both nano-QD LEDs (nano-QLEDs) and nano-perovskite LEDs (nano-PeLEDs), as summarized in Table 1. These developments draw on diverse nanofabrication routes, as outlined in Box 1. Hybrid strategies, such as nanoimprint patterning combined with capillary liquid-bridge-confined assembly, further integrate top–down feature definition with bottom–up material organization to enhance pixel fidelity and produce sharply defined boundaries[19]. Nevertheless, the overall performance of nano-QLEDs remains unbalanced. External quantum efficiencies (EQEs) are typically modest, and operational lifetimes remain far below practical deployment thresholds, which often require T_{90} (the time for luminance to decay to 90% of its initial value) to exceed 10,000 h (ref. 59). No single material platform has yet simultaneously achieved competitive figures of merit across all key metrics; the smallest pixel dimensions, highest EQEs and longest lifetimes are currently distributed across disparate reports, material systems and colour channels. Moreover, sidewall passivation strategies that prove effective for micro-QLEDs become inadequate at the nanoscale, where defect-assisted non-radiative recombination at sidewalls dominates device behaviour[48]. Concurrently, the high current densities required to drive nanoscale emitters induce substantial localized Joule heating, and efficient thermal dissipation becomes progressively more challenging in densely packed arrays[60]. Collectively, these defect- and heat-related phenomena give rise to pronounced efficiency roll-off during device miniaturization. Additionally, precise pixel placement represents a critical bottleneck for nano-QLED technologies. Accumulated misalignments between layers or sub-pixels can engender current leakage and colour crosstalk, presenting a formidable barrier

https://doi.org/10.1038/s41566-026-02010-1

Table 1 | Representative performance parameters of nano-QLEDs and nano-PeLEDs

	Emissive material	PPI	Pixel (μm)	EQE (%)	Luminance (cd m^{-2})	EL peak (nm)	Lifetime (h)	Ref.
QLEDs	CdSe/ZnS	169,333 (monochrome)	0.07	17.0	~10,000	635	T_{90}, 7,969.7 (100 cd m^{-2})	74
	CdSe/ZnS/ZnSe	20,526 (monochrome)	~0.4	23.3	100,471	525	–	73
	CdSe/ZnS	12,700 (monochrome)	0.50	26.1	62,170	630	T_{90}, 65,190 (1,000 cd m^{-2})	75
	CdSe/ZnS	26,075 (monochrome)	0.55	19.5	282,830	635	T_{95}, 4,871 (1,000 cd m^{-2})	97
	CdSe/ZnS	25,400 (monochrome)	~0.5	14.7	262,400	625	–	49
	CdSe/$Cd_xZn_{1-x}Se$/$ZnSe_yS_{1-y}$	15,875 (full-colour)	0.8	20	>10,000	610	T_{80}, 110 (30 mA cm^{-2})	52
	CdSe	23,090 (monochrome)	0.8	16.5	27,861	634	–	70
	InP/ZnSeS	12,700 (monochrome)	1.0	8.3	>4,000	540	T_{90}, 156 (1,000 cd m^{-2})	98
PeLEDs	$FAPbI_3$	127,000 (monochrome)	0.09	20	–	800	–	44
	$CsPbBr_3$ (monochrome)	63,500 (monochrome)	0.18	–	–	–	–	78

Dashes indicate data not reported in the corresponding references.

to large-scale integration and commercial viability[61]. Next, we examine the detailed progress in nano-QLEDs and nano-PeLEDs, and discuss the persistent challenges and prospective solutions for improving device performance.

Nano-QLEDs

Recent progress in QLEDs highlights the particular promise of QDs as emissive materials for nano-LEDs, because their high PLQY, narrow emission bandwidth, colour tunability and solution-processable patternability can support high-colour-purity nanoscale emitters[62]. At the limit of extreme pixel miniaturization, charge injection, interfacial transport and emissive-material stability become increasingly coupled. In nano-QLEDs, interfacial charge accumulation can disrupt the requisite carrier balance, enhancing Auger- or trap-assisted recombination and triggering performance decay under sustained electrical bias. Therefore, the operational stability of nano-QLEDs depends critically on robust QD material designs. The stability of nano-QLEDs is predominantly governed by phase-stabilization kinetics and the chemical robustness of the ligand–shell environment. Ligand strategies involving short amine or thiol ligands, electrochemically inert ligands and crosslinkable ligands can improve QD packing, charge transport, pattern robustness and resistance to carrier-induced degradation[63,64]. Meanwhile, core–shell designs can reduce surface trapping, suppress Auger losses, improve environmental stability, and tune band alignment for balanced injection[65,66]. In addition, recent insights have shifted the focus towards intrinsic structural vulnerabilities. Notably, Zeng and colleagues identified a degradation mechanism originating from the lattice–interface nexus: photo- or thermally induced lattice expansion weakens ionic bonding, thereby lowering ion-migration barriers and accelerating surface oxidation. To circumvent these pathways, a hierarchical-shell strategy—incorporating interbonded $PbSO_4$, SiO_2 and siloxane layers—was developed to simultaneously lock the soft ionic lattice and passivate reactive surface sites (Fig. 3a)[67]. This mechanistically robust framework shifts the stabilization paradigm from merely delaying extrinsic environmental ingress to fundamentally suppressing the intrinsic origins of degradation. The resulting perovskite nanocrystal films exhibit near-unity PLQY and commercially viable stability (T_{90} > 27,000 h under blue-light exposure), establishing lattice–interface interlocking as a universal design principle for the stabilization of soft halide QDs. These material-level designs are particularly important for nano-QLEDs, where reduced pixel volume amplifies QD charging, interfacial quenching and exciton-density-driven losses.

Nanoscale fabrication is not merely a geometric downscaling step, but a critical process that determines whether the designed QD materials can retain their optical and electrical properties in high-density pixel arrays. Recent studies have demonstrated that both nano- and micro-QLEDs can be fabricated by photolithography, electrophoretic deposition, nanoimprinting and transfer printing. Each route exhibits distinct trade-offs in flexibility, resolution, scalability, mildness, cost-effectiveness and throughput when applied to nano-LED manufacturing (Fig. 3b)[68–70]. Photolithography offers CMOS compatibility but can introduce process-induced damage and is increasingly challenged when patterning fragile emitters at deep-subwavelength dimensions. Electrophoretic deposition is attractive for low-cost, large-area coating, yet its stochastic assembly and solvent-rich environment limit pixel precision and pattern uniformity. By contrast, transfer printing enables damage-minimized integration of preformed emissive layers onto flexible, non-planar or heterogeneous substrates, although its serial transfer process can constrain throughput. Nanoimprinting offers a more scalable route for periodic nanoscale arrays, combining reusable moulds, high pattern fidelity and low-cost parallel replication. With continued advances in soft stamps, release layers and emitter-compatible imprinting conditions, nanoimprinting is emerging as a particularly promising strategy for high-throughput nano-LED manufacturing. So far, nano-QLEDs fabricated by transfer printing and nanoimprinting have exhibited excellent device performance and ultrahigh resolution. For example, Meng and colleagues have combined Langmuir–Blodgett film assembly with transfer printing to form highly uniform submicrometre QD patterns, enabling resolutions up to 25,400 PPI (ref. 49).

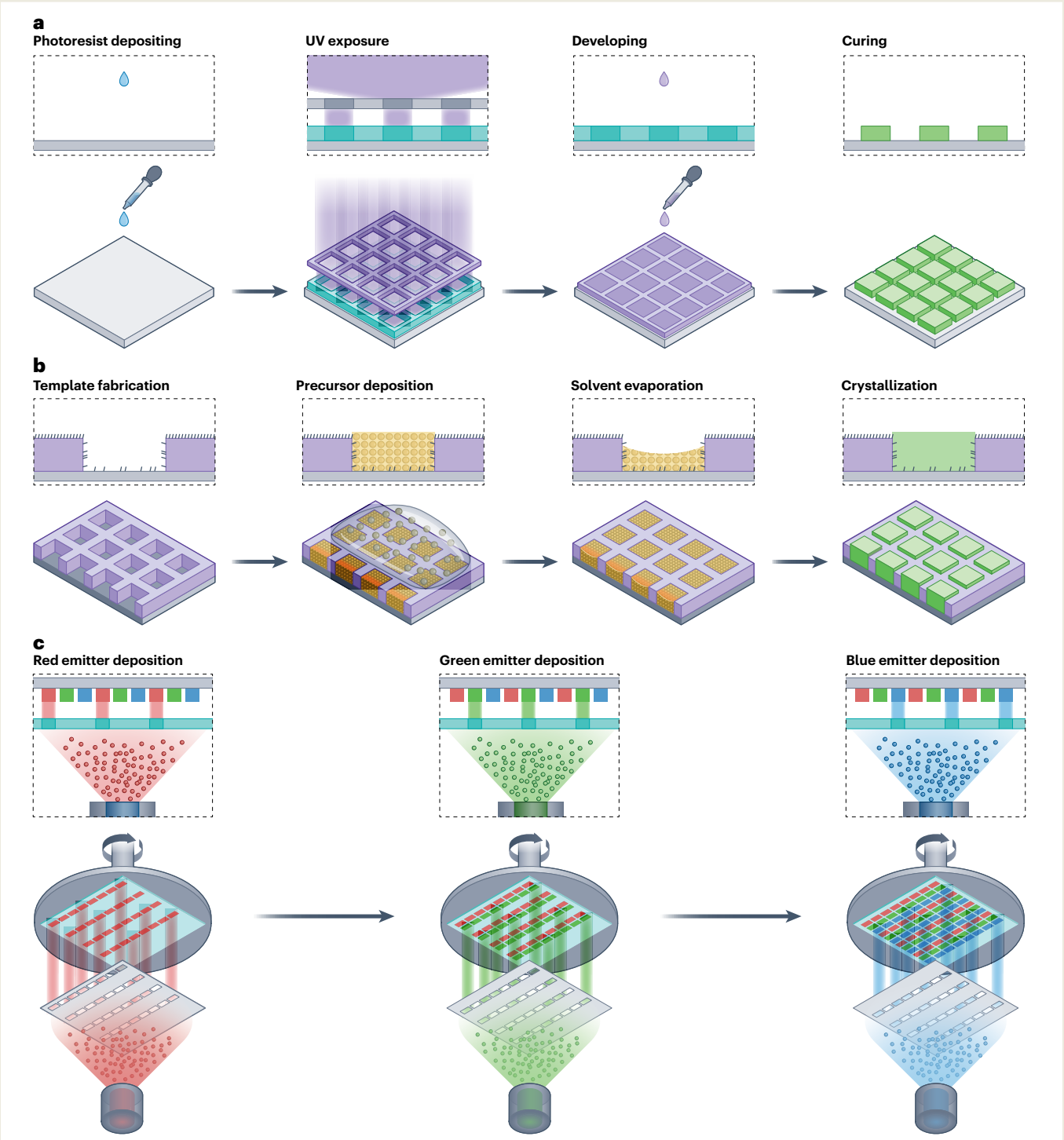
Overcoming the trade-off between high-resolution patterning and high EL efficiency in printed QLEDs requires regulating QD surfaces to simultaneously enhance charge-carrier transport and radiative recombination upon condensation into a solid film. Controlled assembly can reduce film discontinuity, interfacial disorder and leakage pathways in QD emissive layers, thereby maintaining balanced carrier transport within confined pixels[71]. At the same time, improving nanoscale uniformity and structural order suppresses defect- or disorder-assisted non-radiative recombination, allowing injected carriers to recombine radiatively instead of being lost at rough interfaces, grain boundaries or poorly packed domains[72]. Double-layer transfer printing of a QD/ZnO stack using a surface-engineered oxidized polydimethylsiloxane (PDMS) stamp has recently enabled high-definition and flexible/wearable QLEDs. By preserving close contact between the emissive and electron-transport layers, suppressing leakage current and maintaining high EQE in densely patterned pixels, this approach has enabled red green blue (RGB) pixelated patterns at 2,565 PPI and monochromatic patterns at ~20,526 PPI, while simultaneously delivering a very high green-device EQE of 23.3% (ref. 73). Moreover, this strategy highlights transfer printing as an effective route for mechanically compliant and damage-minimized nano-LED integration. Notably, miniaturized pixels with dimensions below 100 nm can considerably

https://doi.org/10.1038/s41566-026-02010-1

BOX 1

Nanofabrication routes for nano-LEDs

Miniaturizing LED pixels into the nanoscale (<1 μm) regime without sacrificing performance is essential for the development of nano-LED technologies. Achieving this goal depends critically on the choice of nanofabrication strategy, which determines pixel fidelity, material integrity and compatibility with large-area integration. The major nanofabrication routes for making nano-LEDs can be classified into three types: top–down patterning, bottom–up fabrication and fine-metal-mask evaporation.



Box Fig. 1 | Nanofabrication routes for nano-LEDs. a, Illustration of top–down photolithography nanofabrication techniques for nano-LEDs. **b**, Illustration of bottom–up templated-assisted growth for nano-LEDs. **c**, Illustration of making nano-OLEDs using fine-metal-deposition evaporation.

(continued from previous page)

Top–down patterning methods start from a continuous film or fully processed device stack and define pixel dimensions by selectively removing materials using techniques such as photolithography, etching and nanoimprinting. Photolithography is one of the most widely used approaches for micro-LED fabrication, owing to its inherent compatibility with silicon complementary metal–oxide–semiconductor (CMOS) platforms (panel **a** in the figure). However, resist coating, solvent exposure, energetic irradiation and plasma etching during this process can damage chemically sensitive emitters, including halide perovskites and organic semiconductors.

Bottom–up fabrication methods define pixels through localized growth, self-assembly or direct deposition rather than material removal. A prominent bottom–up strategy is template-assisted growth, in which prepatterned nanoscale templates confine the nucleation and growth of emissive materials (panel **b** in the figure). These techniques are particularly attractive for solution-processable materials such as QDs, halide perovskites and organic semiconductors.

Fine-metal-mask evaporation is a critical nanofabrication technique for making nano-OLEDs (panel **c** in the figure). In this approach, organic semiconductors are deposited through a patterned metal mask, which defines the pixel geometry during physical vapour deposition. However, whether this strategy can be adapted to other classes of nano-LEDs, such as perovskite- or QD-based devices, remains unknown, owing to differences in material stability, deposition requirements and process compatibility.

increase pixel densities; however, the EL performance of single pixelated nano-QLEDs lags substantially behind that of conventional QLEDs. The performance gap across different emission wavelengths also requires attention.

Beyond the imperatives of device efficiency and operational stability, achieving high-fidelity, full-colour patterning at the nanoscale has remained a challenge over the past decade. This persistent bottleneck is now being addressed through holistic integration strategies that enable the realization of monolithic, full-colour nano-LED arrays. Recent nanoimprint patterning based on capillary self-assembly directly addresses this problem by confining QDs into closely packed emissive monolayers within nanohole arrays, thereby reducing morphology-induced leakage pathways and limiting efficiency loss at sub-100-nm pixel sizes, and enabling full-colour displays (Fig. 3c)[74]. Moreover, the challenge of full-colour nanoscale patterning is not solely a matter of lithographic precision, but also one of charge management within highly confined pixel geometries. Lin and colleagues identified electric-field non-uniformity within patterned microholes as a previously underappreciated loss mechanism in ultrahigh-density devices[75]. By tuning the dielectric constant of the blocking layer to better match that of the QD emissive layer, the edge-field crowding, leakage current and associated non-radiative losses can be suppressed, thereby recovering both efficiency and operational stability at extreme pixel densities. This study provided a new route towards full-colour nano-LED displays that do not suffer the severe performance roll-off typically associated with aggressive downscaling. By contrast, Zhang and colleagues extended the concept of pixelated QLEDs beyond conventional disordered nanocrystal films by introducing laterally coherent QD superlattice thin films as the emissive medium[19]. Through ligand–fluoride co-stabilization of rhombic dodecahedral $CsPbBr_3$ nanocrystals and capillary liquid-bridge confined assembly, researchers obtained ultrathin, spatially registered superlattice pixels that preserve long-range order while remaining compatible with high-resolution device fabrication (Fig. 3d–f). The superlattice architecture reduces energetic disorder, suppresses carrier relaxation into low-energy tail states, narrows the emission linewidth, and strengthens interdot electronic coupling, with temperature-dependent transport further indicating the emergence of band-like behaviour. This strategy also enabled the formation of sharply defined rectangular pixels, rather than rounded emissive domains, reducing optical and electrical crosstalk in high-density nano-LED arrays. These collective effects enabled high efficiency, high brightness and prolonged lifetime in pixelated QLEDs, resulting in video frames captured during real-time animation of a tree swaying in the wind. Collectively, these results underscore the central role of QDs in nano-LED development, highlighting their evolution from patterning-limited proof-of-concept structures to increasingly efficient, scalable and durable nanoscale emissive platforms.

Nano-PeLEDs

PeLEDs have attracted considerable attention in recent years owing to their rapidly increasing device efficiencies, high colour purity and low-cost processing[76,77]. Notably, nano-PeLEDs, with nanoscale pixel dimensions, have exhibited performance comparable to that of conventional PeLEDs, indicating that perovskite emissive materials may be suitable for high-performance nano-PeLEDs. Lian et al. demonstrated the successful downscaling of PeLED pixels to the nanoscale, reaching dimensions as small as ~90 nm and achieving a high pixel density of 127,000 PPI—the smallest reported for any class of LEDs so far (Fig. 4a–c)[44]. Notably, nano-PeLEDs using localized contacts in submicrometre-scale pixels can retain a device performance of ~20% (Fig. 4d,e). Similarly, self-aligned close-spaced sublimation growth of perovskite quantum wires has been used to demonstrate perovskite patterns with 180-nm feature size[78]. This method has also achieved a pixel density of 63,500 PPI for nano-LEDs. Meanwhile, researchers have shown the pixelation of perovskite quantum wires with colour conversion films when integrating with GaInN micro-LED arrays, addressing the need for full-colour micro-displays[78]. These advances outperform conventional GaN-based micro-LEDs, which typically suffer from pronounced efficiency roll-off below 10 µm, although challenges such as operational stability and environmental sensitivity still hinder large-scale commercialization.

Despite these breakthroughs, the practical implementation of perovskite-based nano-emitters is hindered by their intrinsic sensitivity to polar solvents, moisture and chemical exposure. These materials are particularly vulnerable to conventional solution-processing and photolithographic workflows, which can induce surface defects, deleterious ion migration, and interfacial degradation—or even partial dissolution of the emissive layer. As the pixel dimensions shrink, these effects exacerbate non-radiative recombination, leading to severe performance losses. Consequently, establishing fabrication compatibility is paramount for preserving device integrity during pixel downscaling. A recent remote epitaxy strategy offers a route to this compatibility challenge by growing transferable single-crystalline perovskite films through a subnanometre graphene interlayer, thereby avoiding direct solution-patterning damage, eliminating grain-boundary-related losses, relaxing strain and enabling high-brightness micro-LED arrays[79]. To circumvent the risks associated with lithographic chemicals, fine-metal-mask (FMM) evaporation has emerged as a promising dry-processing alternative. A notable example is the work of Marcato and colleagues, who reported a scalable fabrication strategy achieving pixel densities exceeding 84,000 PPI with individual pixel features as small as 100 nm (ref. 80). By employing self-aligned FMM evaporation through nanoapertures patterned into a silicon nitride mask, they demonstrated nano-OLED arrays with EQEs up to 10% at the megapixel scale. Such architectures pave the way for ultracompact light sources in super-resolution imaging, optical sensing and hybrid

https://doi.org/10.1038/s41566-026-02010-1

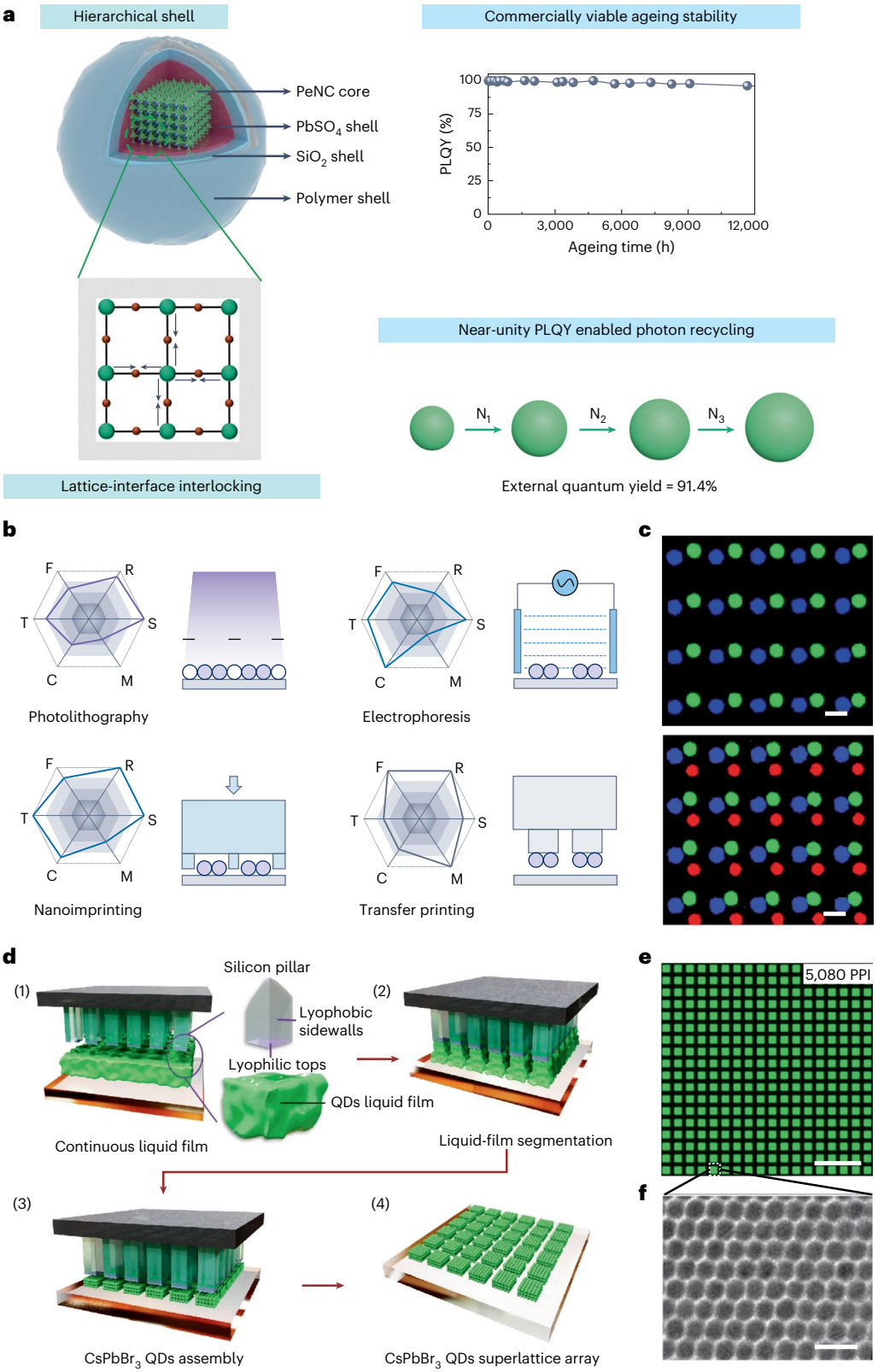


Fig. 3 | Present status of nano-LEDs based on QDs. a, The interbonded $PbSO_4$–SiO_2–polymer layers confine lattice expansion and stabilize the surface of perovskite nanocrystals (PeNCs). Consequently,hierarchical-shell PeNC films maintain near-unity PLQY with efficient photon recycling and achieve an external QL of 91.4%, alongside commercially viable stability (T_{90} > 27,000 h under blue-light exposure). N_1, N_2 and N_3 label the first, second and third photon-recycling events, respectively, each involving photon reabsorption followed by radiative re-emission by PeNCs. **b**, Radar plots of four representative patterning techniques. F, R, S, M, C and T indicate flexibility, resolution, scalability, mildness, cost-effectiveness and throughput. **c**, PL images of GB and RGB patterns composed of multi-colour QD arrays. Scale bars, 10 µm. **d**, Schematic of capillary liquid-bridge confined assembly for patterning PeQD superlattice pixels. **e**, EL image of PeQD superlattice LEDs. Scale bar, 20 µm. **f**, Magnified transmission electron microscopy image of superlattice films showing hexagonal close packed (hcp) structure. Scale bar, 25 nm. Figure adapted with permission from: **a**, ref. 67, AAAS; **c**, ref. 74, Springer Nature Ltd; **d**–**f**, ref. 19, Springer Nature Ltd.

https://doi.org/10.1038/s41566-026-02010-1

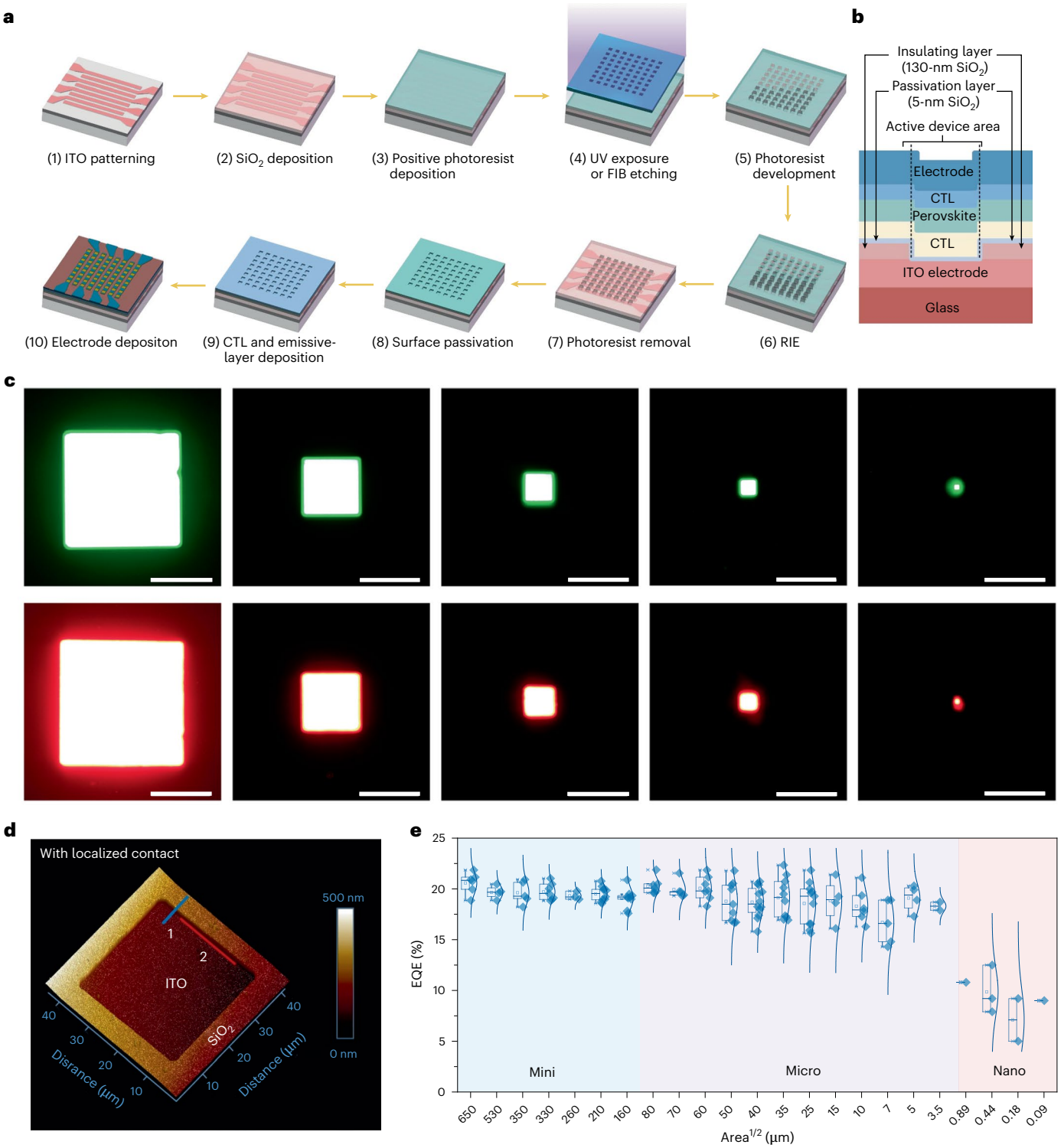


Fig. 4 | Nano-LEDs based on perovskite. a, Fabrication steps for micro- and nano-PeLEDs: (1) ITO patterning by laser etching; (2) deposition of an SiO_2 layer by plasma-enhanced chemical vapour deposition; (3) spin-coating of positive photoresist; (4) UV lithography or dual-beam focused-ion-beam patterning; (5) photoresist development; (6) etching of the SiO_2 layer by reactive ion etching (RIE); (7) photoresist removal; (8) surface passivation by a thin SiO_2 layer (~5 nm); (9) sequential deposition of a charge-transporting layer (CTL) and perovskite; (10) electrode deposition. **b**, Cross-sectional schematic of the PeLED. **c**, Optical microscopic images of working green/red micro-PeLEDs with pixel lengths from 200 μm to ~10 μm, driven at 3.0 V and 3.2 V, respectively. Scale bars, 100 μm. **d**, Atomic force microscope images of the patterned electrodes made with the localized contact method. The blue line labelled 1 and red line labelled 2 indicate the paths used to extract height profiles in the original study. **e**, EQE versus characteristic pixel length plot for near-infrared micro-PeLEDs/nano-PeLEDs. Solid diamonds represent individual experimental EQE values, and red curves show Gaussian fits to the EQE distributions. The box plots and Gaussian fits summarize the mean (open squares), standard deviation, quartiles and extrema of the data. The lower and upper edges of each box indicate the lower quartile (25%) and upper quartile (75%), respectively, defining the interquartile range (25–75%). The horizontal line within each box marks the median (50%), and crosses indicate the minimum and maximum values. Crosses indicate the minimum and maximum values. Cyan, light-purple and pink backgrounds denote the mini-, micro- and nano-PeLED size regimes, respectively. Figure reproduced with permission from: **a**–**e**, ref. 44, Springer Nature Ltd.

https://doi.org/10.1038/s41566-026-02010-1

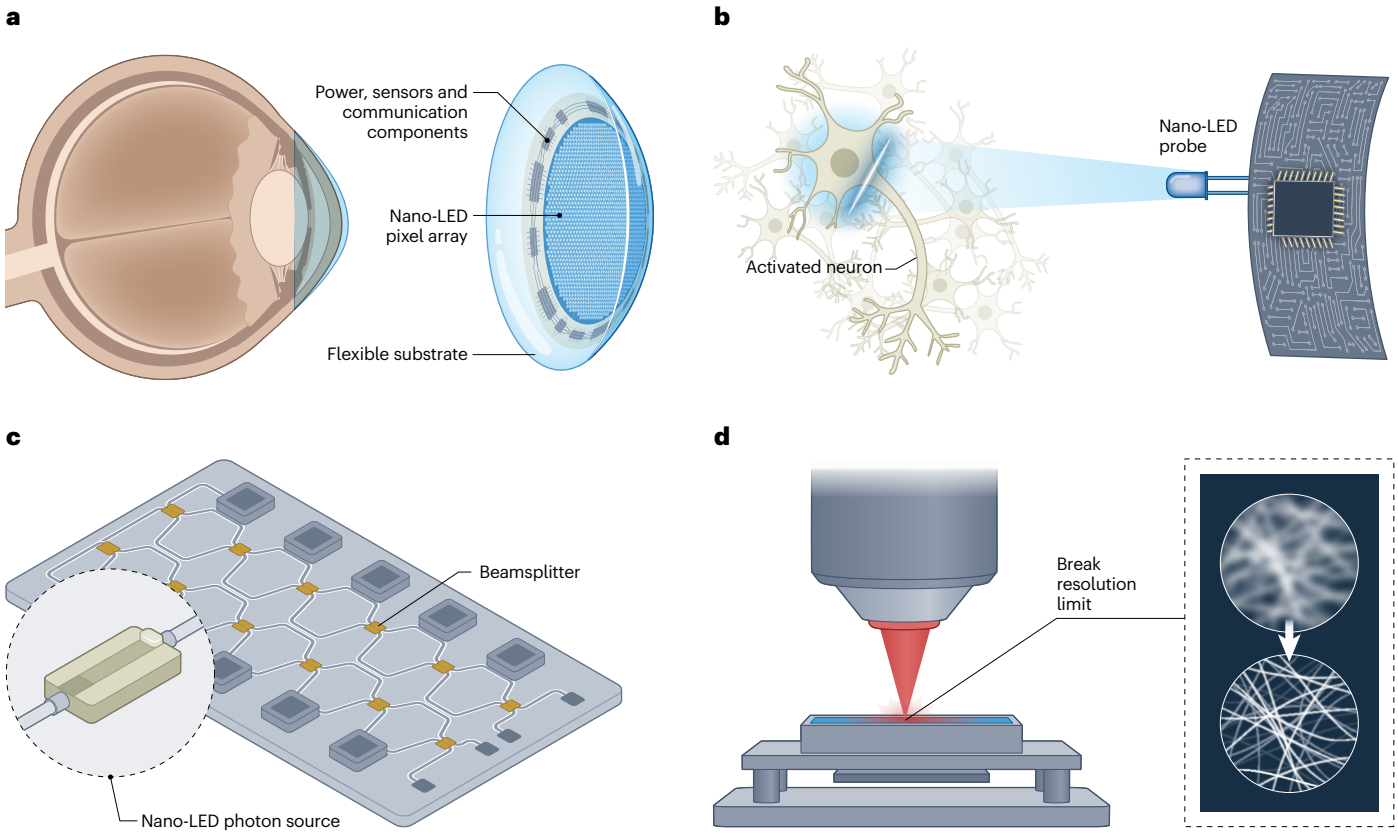


Fig. 5 | Nano-LEDs for cutting-edging applications. a, Illustration of nano-LEDs used for a contact-lens microdisplay. The nano-LED-based contact-lens microdisplay is on the next layer with the power, sensors and communication components. **b**, Illustration showing how a nano-LED probe is used to achieve both high spatial precision and ultrafast modulation for neuroscience. **c**, Illustration of nano-LED-based optical interconnection between chips, circuits and photonic modules. **d**, Nano illumination microscopy based on nano-LED arrays is proposed to push resolutions below the diffraction limit for super-resolution microscopy.

photonic systems. Emerging hybrid approaches, such as transfer printing and direct laser writing, are beginning to bridge this gap, offering a balance between spatial resolution and material integrity. The transition to commercial viability will probably depend on developing perovskite-friendly lithographic resins or refining electrohydrodynamic printing to achieve nanometre-scale precision without compromising the intrinsic optoelectronic properties of the halide semiconductor.

Outlook and perspective

Nano-QLEDs and nano-PeLEDs are poised to extend the performance frontier beyond the reach of conventional micro-LEDs, with their most viable path towards commercialization lying in heterogeneous monolithic integration with environmentally robust GaN-based blue EL arrays. Such hybrid architectures synergize the spectral versatility and scalability of nanocrystals with the material maturity and operational stability of III–V semiconductor platforms. However, transitioning these nano-emitters from laboratory-scale demonstrations to fully integrated micro-displays necessitates synchronized breakthroughs across light emitters, CMOS backplanes and system-level architectures. High-efficiency pixels—characterized by submicrometre pitches and suppressed parasitic leakage—must be co-developed with CMOS backplanes optimized for high-speed, low-power operation at the nanoscale. Bridging this gap demands a holistic co-design framework that spans epitaxial growth, device nanofabrication, and silicon circuitry to reconcile intrinsic mismatches in capacitance, resistance and signal latency. At the system level, the incorporation of on-die machine-learning inference offers a compelling strategy to alleviate data-transfer bottlenecks and enhance computational efficiency.

Beyond displays, we highlight opportunities in biocompatible optoelectronics, super-resolution microscopy and on-chip optical interconnects, where the ultracompact footprint and low-power operation of nano-LEDs could provide distinct advantages. These burgeoning applications underscore the potential of nanoscale emitters to transcend their traditional optoelectronic roles, ultimately catalysing a paradigm shift in our ability to manipulate and interact with light at the ultimate limit of miniaturization. We also propose some key strategies for improving nano-LED performance.

Nano-LEDs for biocompatible optoelectronics

At the frontier of human–machine interaction, contact-lens displays represent a daring goal in optoelectronics-inspired neuroscience: digital imagery that merges seamlessly with natural vision. Nano-LED arrays—with electroluminescent pixels well below the diffraction limit—can deliver submicrometre-pitch emitters and thus ultrahigh-PPI micro-displays small enough to be embedded in a contact lens. Unlike conventional augmented reality (AR)/VR headsets, which depend on bulky optical trains, such a lens could project images directly onto the retina, yielding a truly immersive retinal display. Mojo Vision's recent prototypes (Fig. 5a) provide an early proof of concept[81,82]. Nonetheless, the device performance and stability of nano-LEDs remain limited, and ongoing efforts are thus focused on pushing both metrics to the next level. For example, one approach is to enhance the performance of wearable, stretchable nano-LEDs by adopting biocompatible processing techniques. Soft-contact optical lithography is thought to bridge the gap between nano-LEDs and implantable bio-integrated optoelectronics in neuroscience. By replacing rigid quartz masks with transparent, elastomeric PDMS moulds, this approach enables high-resolution

nanoscale patterns directly on soft and curved substrates[83–85]. In addition, new emissive materials that go beyond traditional III–V semiconductors—such as biocompatible materials that are promising for retinal electronic paper—offer an alternative for contact-lens displays[86].

Beyond contact-lens displays, nano-LED probes could potentially improve spatial precision and response rates in neuroscience (Fig. 5b). Inspired by optogenetic control of genetically targeted neurons, high-speed nano-LEDs should enable modulation of defined neuronal populations on millisecond timescales[87]. So far, micro-LED arrays have already enabled localized and depth-resolved neural photo-stimulation using compact, addressable light sources. For example, a glass microneedle optrode array integrated with 181 micro-LEDs has been developed for in vivo optogenetic stimulation in large mammals, enabling irradiances of >80 mW mm^{-2} per site[88]. If nano-LED arrays can be deployed in this emerging field, they should enhance overall performance. Furthermore, nano-LEDs can provide subcellular-level spatial resolution in neuromodulation and deliver highly localized optical signals with minimal power consumption and heat generation, thereby reducing tissue heating and minimizing crosstalk between adjacent neurons. This is particularly important for deep-brain implantation, where the American Association for Advancement of Medical Devices stipulate that the temperature increases induced by stimulation should be less than 2 °C to avoid damage to neural tissue[89,90]. These combined capabilities make nano-LEDs especially attractive for probing higher-order brain functions—memory encoding, recall, decision-making and multisensory integration.

Nano-LEDs can serve not only as localized light sources for stimulation or sensing in biocompatible optoelectronics, but also as miniature optical interconnects that link biological tissues with electronic or photonic systems. Their compact footprint, low-power operation and spatially confined emission enable optical signals to be delivered, modulated and transmitted at soft biointerfaces, providing a route for localized communication with biological tissues or for short-distance signal transfer between chips, circuits and photonic modules (Fig. 5c)[91,92].

Super-resolution microscopy

Nano-LEDs can generate highly localized light fields with spatial features approaching or even below the emission wavelength[93,94]. This intrinsic property positions nano-LEDs as an attractive light source for super-resolution microscopy based on near-field optical microscopy (SNOM). Indeed, attempts have already been made to integrate nano-LEDs at the apex of a SNOM probe, and such integrated tips have demonstrated optical and topographic resolutions of ~400 nm and ~50 nm, respectively[95]. In addition to SNOM, nano illumination microscopy (NIM) has also recently been proposed as a complementary strategy to improve resolution and surpass the diffraction limit (Fig. 5d)[96]. In NIM, an array of nano-LEDs is expected to be placed in close proximity to the specimen, with each nano-LED acting as an individually addressable, localized illumination source. This architecture shifts the resolution bottleneck from the detector to the illumination source, making the imaging performance predominantly dependent on the nano-LED size and pitch, while reducing the constraints on sensor pixel size and fill factor. Simulations indicate that the achievable resolution scales with the nano-LED size rather than being strictly limited by the detection components, thereby offering a route to surpass the Abbe diffraction limit. Overall, nano-LEDs provide localized, tunable illumination directly at the nanoscale, thereby holding the potential to advance super-resolution microscopy.

Key strategies for nano-LED performance improvement

Efficiency loss and degradation in nano-LEDs arise from coupled processes involving surfaces, charge transport and thermal instabilities. Sidewall defects cause unwanted non-radiative recombination, which is further activated by unbalanced carrier injection and Joule heating. Breaking this feedback loop requires coordinated materials and device design rather than isolated optimization. Robust surface chemistry is needed to stabilize exposed QD or perovskite sidewalls through stronger ligand binding, defect-tolerant compositions, crosslinked passivation networks or inorganic shell/barrier layers. Meanwhile, balanced carrier injection should be achieved by matching electron and hole transport, tuning interfacial energy levels, suppressing leakage currents, and confining recombination away from defective boundaries. Lowering the operating voltage and limiting resistive losses are key to reducing Joule heating. For device fabrication, environmentally friendly, bio-inspired patterning and nanofabrication represent a promising direction towards achieving efficient nano-LEDs, mitigating sidewall-related performance losses. Through such integrated control of sidewall passivation, charge balance and thermal management, nano-LEDs can move towards higher efficiency, longer operational stability and scalable high-density integration. Future research can be advanced through novel materials by leveraging deep learning and AI-accelerated materials discovery. Furthermore, the design of high-resolution nanoscale pixel arrays can be optimized by balancing electrical and optical properties through machine learning-assisted optoelectronic pattern design.

References

1. Han, H.-V. et al. Resonant-enhanced full-color emission of quantum-dot-based micro LED display technology. *Opt. Express* **23**, 32504–32515 (2015).
2. Pal, D., López, T. & Koenderink, A. F. Metasurface-based phosphor-converted micro-LED architecture for displays—creating guided modes for enhanced directionality. *ACS Nano* **19**, 1238–1250 (2025).
3. Anwar, A. R. et al. Recent progress in micro-LED-based display technologies. *Laser Photon. Rev.* **16**, 2100427 (2022).
4. Tan, G. et al. Foveated imaging for near-eye displays. *Opt. Express* **26**, 25076–25085 (2018).
5. Lin, C.-C. et al. The micro-LED roadmap: status quo and prospects. *J. Phys. Photon.* **5**, 042502 (2023).
6. Park, J.-H., Pristovsek, M., Amano, H. & Seong, T.-Y. Recent advances in micro-pixel light emitting diode technology. *Appl. Phys. Rev.* **11**, 021319 (2024).
7. Mikulics, M. et al. Nano-light-emitting-diodes based on InGaN mesoscopic structures for energy saving optoelectronics. *Appl. Phys. Lett.* **109**, 041103 (2016).
8. Marso, M. et al. InGaN nano-LEDs for energy saving optoelectronics. In *Proc. 10th International Conference on Advanced Semiconductor Devices and Microsystems* (eds Breza, J., Donoval, D. & Vavrinsky, E.) 1–4 (IEEE, 2014).
9. Romeira, B., Figueiredo, J. M. L. & Javaloyes, J. NanoLEDs for energy-efficient and gigahertz-speed spike-based sub-λ neuromorphic nanophotonic computing. *Nanophotonics* **9**, 4149–4162 (2020).
10. Owen-Newns, D., Robertson, J., Hejda, M. & Hurtado, A. GHz rate neuromorphic photonic spiking neural network with a single vertical-cavity surface-emitting laser (VCSEL). *IEEE J. Sel. Top. Quantum Electron.* **29**, 1–10 (2022).
11. Liu, Z. et al. Advanced technologies in InGaN micro-LED fabrication to mitigate the sidewall effect. *Light Sci. Appl.* **14**, 64 (2025).
12. Kim, T. S. et al. Future trends of display technology: micro-LEDs toward transparent, free-form and near-eye displays. *Light Sci. Appl.* **14**, 335 (2025).
13. Wu, C., Wang, K., Zhang, Y., Zhou, X. & Guo, T. Emerging nanopixel light-emitting displays: significance, challenges and prospects. *J. Phys. Chem. Lett.* **12**, 3522–3527 (2021).
14. Murawski, C., Leo, K. & Gather, M. C. Efficiency roll-off in organic light-emitting diodes. *Adv. Mater.* **25**, 6801–6827 (2013).
15. Huang, Y., Hsiang, E.-L., Deng, M.-Y. & Wu, S.-T. Mini-LED, micro-LED and OLED displays: present status and future perspectives. *Light Sci. Appl.* **9**, 105 (2020).

16. Protesescu, L. et al. Nanocrystals of cesium lead halide perovskites ($CsPbX_3$, X=Cl, Br and I): novel optoelectronic materials showing bright emission with wide color gamut. *Nano Lett.* **15**, 3692–3696 (2015).
17. Zhang, S. et al. Wafer-scale fabrication of CMOS-compatible trapping-mode infrared imagers with colloidal quantum dots. *ACS Photonics* **10**, 673–682 (2023).
18. Shang, Y. & Ning, Z. Colloidal quantum-dots surface and device structure engineering for high-performance light-emitting diodes. *Natl Sci. Rev.* **4**, 170–183 (2017).
19. Zhang, C. et al. Pixelated quantum-dot superlattice LEDs. *Nature* **652**, 1173–1180 (2026).
20. Wang, N. et al. Perovskite light-emitting diodes based on solution-processed self-organized multiple quantum wells. *Nat. Photon.* **10**, 699–704 (2016).
21. Romeira, B. & Fiore, A. Physical limits of NanoLEDs and nanolasers for optical communications. *Proc. IEEE* **108**, 735–748 (2020).
22. Huang, K. C. Y. et al. Electrically driven subwavelength optical nanocircuits. *Nat. Photon.* **8**, 244–249 (2014).
23. Schubert, M. et al. Monitoring contractility in cardiac tissue with cellular resolution using biointegrated microlasers. *Nat. Photon.* **14**, 452–458 (2020).
24. Gu, W., Wang, L., Wang, X., Zhao, C. & Guan, S. Large-scale, high-density microLED array-based optogenetic device for neural stimulation and recording. *Nano Lett.* **24**, 15252–15259 (2024).
25. Dusanowski, Ł et al. Purcell-enhanced and indistinguishable single-photon generation from quantum dots coupled to on-chip integrated ring resonators. *Nano Lett.* **20**, 6357–6363 (2020).
26. Tsujino, K. et al. 25-2: Invited paper: ultra-high-resolution nanoLED panel for AR/VR by UV patterning technology. *SID Symp. Dig. Tech. Pap.* **53**, 291–294 (2022).
27. Sharif Azadeh, S. et al. Microcantilever-integrated photonic circuits for broadband laser beam scanning. *Nat. Commun.* **14**, 2641 (2023).
28. Bharadwaj, P., Deutsch, B. & Novotny, L. Optical antennas. *Adv. Opt. Photon.* **1**, 438–483 (2009).
29. Sauvan, C., Hugonin, J. P., Maksymov, I. S. & Lalanne, P. Theory of the spontaneous optical emission of nanosize photonic and plasmon resonators. *Phys. Rev. Lett.* **110**, 237401 (2013).
30. Curto, A. G. et al. Unidirectional emission of a quantum dot coupled to a nanoantenna. *Science* **329**, 930–933 (2010).
31. Wang, X., Zhao, X., Takahashi, T., Ohori, D. & Samukawa, S. $3.5\times3.5\,\mu m^2$ GaN blue micro-light-emitting diodes with negligible sidewall surface nonradiative recombination. *Nat. Commun.* **14**, 7569 (2023).
32. Shin, Y. et al. Investigation and direct observation of sidewall leakage current of InGaN-based green micro-light-emitting diodes. *Opt. Express* **30**, 21065–21074 (2022).
33. Xu, Y., Cui, J., Hu, Z., Gao, X. & Wang, L. Pixel crosstalk in naked-eye micro-LED 3D display. *Appl. Opt.* **60**, 5977–5983 (2021).
34. Chen, J. et al. Optical crosstalk reduction of InGaN micro-LED array based on a reflective wall design for display applications. *Opt. Lett.* **51**, 476–479 (2026).
35. Yapparov, R. et al. Origin of reduced efficiency in GaN-based micro-LEDs studied by scanning near-field optical microscopy. *Appl. Phys. Lett.* **126**, 201102 (2025).
36. Shen, H.-T., Weisbuch, C., Speck, J. S. & Wu, Y.-R. Three-dimensional modeling of minority-carrier lateral diffusion length including random alloy fluctuations in (In, Ga)N and (Al, Ga)N single quantum wells. *Phys. Rev. Appl.* **16**, 024054 (2021).
37. Zou, C., Liu, Y., Ginger, D. S. & Lin, L. Y. Suppressing efficiency roll-off at high current densities for ultra-bright green perovskite light-emitting diodes. *ACS Nano* **14**, 6076–6086 (2020).
38. Asad, M., Li, Q., Sachdev, M. & Wong, W. S. Thermal and optical properties of high-density GaN micro-LED arrays on flexible substrates. *Nano Energy* **73**, 104724 (2020).
39. Li, Z. et al. Highly bright perovskite light-emitting diodes enabled by retarded Auger recombination. *Nat. Commun.* **16**, 927 (2025).
40. Ingram, G. L., Zhao, Y.-B. & Lu, Z.-H. Exciton-triggered luminance degradation of organic light-emitting diodes. *Org. Electron.* **69**, 160–163 (2019).
41. McIsaac, A. R. et al. Investigation of external quantum efficiency roll-off in OLEDs using the mean-field steady-state kinetic model. *J. Phys. Chem. C* **124**, 14424–14431 (2020).
42. van der Zee, B., Li, Y., Wetzelaer, G.-J. A. H. & Blom, P. W. M. Triplet-polaron-annihilation-induced degradation of organic light-emitting diodes based on thermally activated delayed fluorescence. *Phys. Rev. Appl.* **18**, 064002 (2022).
43. Emon, D. H. & Kim, H. K. Suspended nano scale QD-OLED on Si substrate. In *Proc. 2017 IEEE 17th International Conference on Nanotechnology* (*IEEE-NANO*) 974–978 (IEEE, 2017).
44. Lian, Y. et al. Downscaling micro- and nano-perovskite LEDs. *Nature* **640**, 62–68 (2025).
45. Lin, B.-C. et al. Advantages of blue LEDs with graded-composition AlGaN/GaN superlattice EBL. *IEEE Photon. Technol. Lett.* **25**, 2062–2065 (2013).
46. Zhang, M., Bhattacharya, P. & Guo, W. InGaN/GaN self-organized quantum dot green light emitting diodes with reduced efficiency droop. *Appl. Phys. Lett.* **97**, 011103 (2010).
47. Brandt, O. et al. Carrier diffusion in GaN: a cathodoluminescence study. II. Ambipolar versus exciton diffusion. *Phys. Rev. Appl.* **17**, 024018 (2022).
48. Lee, J., Chiu, Y. C. & Bayram, C. Efficiency cliff in scaling InGaN light-emitting diodes down to submicron. *Appl. Phys. Lett.* **126**, 242101 (2025).
49. Meng, T. et al. Ultrahigh-resolution quantum-dot light-emitting diodes. *Nat. Photon.* **16**, 297–303 (2022).
50. Sheen, M. et al. Highly efficient blue InGaN nanoscale light-emitting diodes. *Nature* **608**, 56–61 (2022).
51. Park, D. et al. High-performance blue OLED using multiresonance thermally activated delayed fluorescence host materials containing silicon atoms. *Nat. Commun.* **14**, 5589 (2023).
52. Hahm, D. et al. Direct patterning of colloidal quantum dots with adaptable dual-ligand surface. *Nat. Nanotechnol.* **17**, 952–958 (2022).
53. Jang, E. & Jang, H. Quantum dot light-emitting diodes. *Chem. Rev.* **123**, 4663–4692 (2023).
54. Lim, J. et al. Influence of shell thickness on the performance of light-emitting devices based on $CdSe/Zn_{1-x}Cd_xS$ core/shell heterostructured quantum dots. *Adv. Mater.* **26**, 8034–8040 (2014).
55. Shu, L. et al. Highly efficient blue light-emitting diodes based on perovskite film with vertically graded bandgap and organic grain boundary passivation shells. *Adv. Funct. Mater.* **33**, 2306570 (2023).
56. Lei, Y. et al. Perovskite superlattices with efficient carrier dynamics. *Nature* **608**, 317–323 (2022).
57. D'Amato, M., Tan, Q. Y., Glorieux, Q., Bramati, A. & Soci, C. Color-tunable mixed-cation perovskite single photon emitters. *ACS Photonics* **10**, 197–205 (2023).
58. Quan, L. N., García, de Arquer, F. P., Sabatini, R. P. & Sargent, E. H. Perovskites for light emission. *Adv. Mater.* **30**, 1801996 (2018).
59. Jarikov, V. V. et al. Operating longevity of organic light-emitting diodes with perylene derivatives as aggregating light-emitting-layer additives: expansion of the emission zone. *J. Appl. Phys.* **100**, 094907 (2006).
60. Konoplev, S. S., Bulashevich, K. A. & Karpov, S. Y. From large-size to micro-LEDs: scaling trends revealed by modeling. *Phys. Status Solidi a* **215**, 1700508 (2018).

61. Yoon, S. U., Hwangbo, Y., Jang, B., Kim, H. D. & Kim, J. H. Transfer of micro-LEDs with roll-based direct overlay alignment for manufacturing transparent displays. *Adv. Electron. Mater.* **10**, 2400236 (2024).
62. Zhang, X. et al. Nanostructured materials for next-generation display technology. *Nat. Rev. Electr. Eng.* **2**, 263–276 (2025).
63. Pu, C. et al. Electrochemically-stable ligands bridge the photoluminescence–electroluminescence gap of quantum dots. *Nat. Commun.* **11**, 937 (2020).
64. Chen, Z. et al. Rigid crosslinker-assisted nondestructive direct photolithograph for patterned QLED displays. *Light Sci. Appl.* **14**, 251 (2025).
65. Won, Y.-H. et al. Highly efficient and stable InP/ZnSe/ZnS quantum dot light-emitting diodes. *Nature* **575**, 634–638 (2019).
66. Cao, W. et al. Highly stable QLEDs with improved hole injection via quantum dot structure tailoring. *Nat. Commun.* **9**, 2608 (2018).
67. Zeng, Q. et al. A hierarchical shell locks and stabilizes perovskite nanocrystals with near-unity quantum yield. *Science* **391**, eady1370 (2026).
68. Houtepen, A. et al. Colloidal quantum dots for optoelectronics. *Nat. Rev. Methods Primers* **5**, 42 (2025).
69. Zhu, X. et al. Broadband perovskite quantum dot spectrometer beyond human visual resolution. *Light Sci. Appl.* **9**, 73 (2020).
70. Luo, C. et al. Ultrahigh-resolution, high-fidelity quantum dot pixels patterned by dielectric electrophoretic deposition. *Light Sci. Appl.* **13**, 273 (2024).
71. Jia, Y. et al. Long-range order enhance performance of patterned blue quantum dot light-emitting diodes. *Nat. Commun.* **16**, 7643 (2025).
72. Li, H. et al. Highly efficient light-emitting diodes via self-assembled InP quantum dots. *Nat. Commun.* **16**, 4257 (2025).
73. Yoo, J. et al. Highly efficient printed quantum dot light-emitting diodes through ultrahigh-definition double-layer transfer printing. *Nat. Photon.* **18**, 1105–1112 (2024).
74. Cao, W. et al. Ultrahigh-resolution nanoimprint patterning of quantum-dot light-emitting diodes via capillary self-assembly. *Nat. Photon.* **20**, 301–309 (2026).
75. Lin, L. et al. Nanoscale transfer-printed full-colour ultrahigh-resolution quantum dot LEDs. *Nature* **652**, 349–358 (2026).
76. Han, T.-H. et al. A roadmap for the commercialization of perovskite light emitters. *Nat. Rev. Mater.* **7**, 757–777 (2022).
77. Yuan, S. et al. Efficient blue electroluminescence from reduced-dimensional perovskites. *Nat. Photon.* **18**, 425–431 (2024).
78. Zhang, Q. et al. Pixelation of perovskite quantum wire thin films with 0.18-μm features and 63,500-ppi pixel density. *Sci. Adv.* **11**, eadu3840 (2025).
79. Yuan, M. et al. Remote epitaxial crystalline perovskites for ultrahigh-resolution micro-LED displays. *Nat. Nanotechnol.* **20**, 381–387 (2025).
80. Marcato, T. et al. Scalable nanopatterning of organic light-emitting diodes beyond the diffraction limit. *Nat.Photon.* **20**, 31–39 (2026).
81. Martin, P. S. Mojo vision nanoLEDs for invisible computing. In *Light-Emitting Devices, Materials and Applications XXIV* Vol. 11302 (eds Kim, J. K., Krames, M. R. & Strassburg, M.) 1130204 (SPIE, 2020).
82. Martin, P. S. 25–4: contact lens embedded microLED displays. *SID Symp. Dig. Tech. Pap.* **53**, 1521–1523 (2022).
83. Lee, T.-W. et al. Soft-contact optical lithography using transparent elastomeric stamps and application to nanopatterned organic light-emitting devices. *Adv. Funct. Mater.* **15**, 1435–1439 (2005).
84. Lee, T.-W., Zaumseil, J., Kim, S. H. & Hsu, J. W. P. High-efficiency soft-contact-laminated polymer light-emitting devices with patterned electrodes. *Adv. Mater.* **16**, 2040–2045 (2004).
85. Lee, T.-W., Zaumseil, J., Bao, Z., Hsu, J. W. P. & Rogers, J. A. Organic light-emitting diodes formed by soft contact lamination. *Proc. Natl Acad. Sci. USA* **101**, 429–433 (2004).
86. Santosa, A. S. S. et al. Video-rate tunable colour electronic paper with human resolution. *Nature* **646**, 1089–1095 (2025).
87. Boyden, E. S., Zhang, F., Bamberg, E., Nagel, G. & Deisseroth, K. Millisecond-timescale, genetically targeted optical control of neural activity. *Nat. Neurosci.* **8**, 1263–1268 (2005).
88. McAlinden, N. et al. Multisite microLED optrode array for neural interfacing. *Neurophotonics* **6**, 035010 (2019).
89. Fujii, T. & Ibata, Y. Effects of heating on electrical activities of guinea pig olfactory cortical slices. *Pflügers Arch.* **392**, 257–260 (1982).
90. Goldstein, L. S., Dewhirst, M. W., Repacholi, M. & Kheifets, L. Summary, conclusions and recommendations: adverse temperature levels in the human body. *Int. J. Hyperthermia* **19**, 373–384 (2003).
91. Deshpande, S., Heo, J., Das, A. & Bhattacharya, P. Electrically driven polarized single-photon emission from an InGaN quantum dot in a GaN nanowire. *Nat. Commun.* **4**, 1675 (2013).
92. Zeng, H. et al. Quantum light generation based on GaN microring toward fully on-chip source. *Phys. Rev. Lett.* **132**, 133603 (2024).
93. Kluczyk-Korch, K. et al. Individually switchable InGaN/GaN nano-LED arrays as highly resolved illumination engines. *Electronics* **10**, 1829 (2021).
94. Kluczyk-Korch, K. et al. Optical design of InGaN/GaN nanoLED arrays on a chip: toward: highly resolved illumination. *Nanotechnology* **32**, 105203 (2021).
95. Hoshino, K., Gopal, A. & Zhang, X. Near-field scanning nanophotonic microscopy—breaking the diffraction limit using integrated nano light-emitting probe tip. *IEEE J. Sel. Top. Quantum Electron.* **15**, 1393–1399 (2009).
96. Franch, N. et al. Nano illumination microscopy: a technique based on scanning with an array of individually addressable nanoLEDs. *Opt. Express* **28**, 19044–19057 (2020).
97. Zhong, C. et al. High-performance, high-resolution quantum dot light-emitting diodes with self-assembly single-molecular interface modification. *Nano Lett.* **24**, 14125–14132 (2024).
98. Yang, J. et al. Nondestructive photopatterning of heavy-metal-free quantum dots. *Adv. Mater.* **34**, 2205504 (2022).

Acknowledgements

We thank Z.-H. Lu for insightful discussions and suggestions. D.L. was supported by the National Natural Science Foundation of China (grant no. 52573266) and Fundamental Research Funds for the Central Universities (grant no. 501RCQD2025158003). T.-W.L. was supported by the National Research Foundation of Korea (NRF), funded by the Ministry of Science, ICT & Future Planning (grant no. RS-2025-00560490). W.Y. was supported by the National Natural Science Foundation of China (grant no. 12574467) and Fundamental Research Funds for the Central Universities (grant no. 501XYGG2025158009). W.Y. and D.L. were supported by the State Key Laboratory of Alternate Electrical Power System with Renewable Energy Sources (grant no. LAPS25005). A.R. was supported by the National Natural Science Foundation of China (grant no. 52472148). X.Y. was supported by the China Postdoctoral Science Foundation (grant nos. BX20250354 and 2025M770177) and Young Elite Scientists Sponsorship Program of the Beijing High Innovation Plan (grant no. 20250791).

Author contributions

W.Y., A.R., X.Y. and H.W. researched most of the data and wrote the draft. D.L. revised the manuscript and supervised the project. T.-W.L. contributed to manuscript editing and comments.

Competing interests

The authors declare no competing interests.

Additional information

Correspondence and requests for materials should be addressed to Tae-Woo Lee or Deying Luo.

Peer review information *Nature Photonics* thanks Yuchen Wu and the other, anonymous, reviewer(s) for their contribution to the peer review of this work.

Reprints and permissions information is available at www.nature.com/reprints.

Publisher's note Springer Nature remains neutral with regard to jurisdictional claims in published maps and institutional affiliations.

Springer Nature or its licensor (e.g. a society or other partner) holds exclusive rights to this article under a publishing agreement with the author(s) or other rightsholder(s); author self-archiving of the accepted manuscript version of this article is solely governed by the terms of such publishing agreement and applicable law.

© Springer Nature Limited 2026